DOI: 10.1002/ejic.200600479

Syntheses, Characterization, and X-ray Crystal Structures of Mono-Lacunary Dawson Polyoxometalate-Based Organosilyl Complexes

Chika Nozaki Kato,[a] Yuhki Kasahara,[a] Kunihiko Hayashi,[a] Asuka Yamaguchi,[a] Takeshi Hasegawa,[a] and Kenji Nomiya*[a]

Keywords: Silicon / Polyoxometalates / X-ray diffraction / Tungsten

The syntheses and crystal structures of a series of organosilyl polyoxotungstate derivatives with the Dawson monovacant phosphotungstate $[\alpha_2\text{-}P_2W_{17}O_{61}]^{10-}$ are described. The polyoxometalates $(Me_2NH_2)_5H[\alpha_2\text{-}P_2W_{17}O_{61}\{O[Si(CH_2)_3SH]_2\}]\cdot 6H_2O$ (Me_2NH_2-**1**), $(Me_2NH_2)_6[\alpha_2\text{-}P_2W_{17}O_{61}\{O[Si(CH_2)_3SCN]_2\}]\cdot 3H_2O$ (Me_2NH_2-**2**), and $(Me_2NH_2)_6[\alpha_2\text{-}P_2W_{17}O_{61}\{O(SiPh)_2\}]\cdot 4H_2O$ (Me_2NH_2-**3**) were obtained as analytically pure, homogeneous yellow crystals by the reaction of monolacunary Dawson polyoxotungstate with $HS(CH_2)_3Si(OMe)_3$, $NCS(CH_2)_3Si(OEt)_3$, and $PhSiCl_3$, respectively, in an HCl/water/acetonitrile mixed solution or a water/acetonitrile mixed solution, followed by crystallization from water in the dark. Single-crystal X-ray structure analyses revealed that the four-coordinate –Si–O–Si– bonding of the organosilyl groups $\{O[Si(CH_2)_3SH]_2\}$, $\{O[Si(CH_2)_3SCN]_2\}$, and $\{O(SiPh)_2\}$ is attained through four oxygen atoms in the mono-lacunary site of the polyanion, resulting in an overall C_1 symmetry for Me_2NH_2-**1** and Me_2NH_2-**2** and C_s symmetry for Me_2NH_2-**3**. In the molecular structures of Me_2NH_2-**1** and Me_2NH_2-**2**, a unique configuration of the organosilyl groups is observed in the solid state, i.e. the equatorial and axial bonding of each of the two $HS(CH_2)Si$ moieties in the $\{O[Si(CH_2)_3SH]_2\}$ group for Me_2NH_2-**1** and the two $NCS(CH_2)_3Si$ moieties oriented in a *syn* fashion in the $\{O[Si(CH_2)_3SCN]_2\}$ group for Me_2NH_2-**2**. The characterization of Me_2NH_2-(**1**–**3**) was accomplished by elemental analysis, TG/DTA, and FT-IR, solution (^1H, ^{13}C, and ^{31}P) NMR, and solid-state ^{13}C NMR spectroscopy.

Introduction

Polyoxometalates (POMs) have attracted considerable attention because of their extreme versatility and unique range of properties, including catalytic and biological activities and/or photo- and electrochromism.[1] The introduction of organic groups into POMs is an efficient technology to significantly increase the number of organic–inorganic hybrid compounds and thus to improve their properties. For example, organostannyl derivatives such as $[TW_{11}O_{39}(SnCH_2CH_2X)]^{n-}$ [T (isomer) = Si (α), Ge (α), Ga (a mixture of α and β); X = COOH, $COOCH_3$, $CONH_2$, CN; *n* = 5,6],[2] $[\alpha\text{-}XW_{11}O_{39}(SnR)]^{n-}$ [X = P, As, Si; R = Me, *n*Bu, Ph, $CH_2C_6H_5$, $(CH_2)_3Br$, $(CH_2)_4Cl$, $(CH_2)_{11}CH_3$, $(CH_2)_6Br$, $C_{27}H_{45}$, CN; *n* = 5,6],[3] $[\alpha_2\text{-}X_2W_{17}O_{61}(SnR)]^{7-}$ [X = P, As; R = Me, *n*Bu, Ph, $(CH_2)_{11}CH_3$],[3] $[\alpha_2\text{-}P_2W_{17}O_{61}(SnCH_2R)]^{7-}$ (R = CH_2COOH, CH_2COOEt, $CH{=}CH_2$, CH_2CHO),[4] $[\alpha_1\text{-}P_2W_{17}O_{61}(SnCH_2R)]^{7-}$ (R = CH_2COOH, CH_2COOEt, $CH_2COOMenthyl$),[4] $[(\beta\text{-}APW_9O_{34})_2(RSnOH)_3]^{12-}$ (R = Ph, Bu),[5] $[\alpha\text{-}P_2W_{15}O_{59}(RSn)_3]^{9-}$ (R = Ph, Bu),[5] $[SiW_9O_{37}(RSn)_3]^{7-}$ (R, isomer: Ph, α; *n*Bu, α; Ph, β; *n*Bu, β),[6] and $[(SiW_9O_{34})_2(RSnOH)_3]^{14-}$ (R, isomer: Ph, α; *n*Bu, α; Ph, β; *n*Bu, β),[6] and $[(\gamma\text{-}SiW_{10}O_{36})_2(PhSnOH)_2]^{10-}$;[7] organophosphonyl derivatives such as $[\alpha\text{-}A\text{-}PW_9O_{34}(RPO)_2]^{5-}$ (R = Et, *n*Bu, *t*Bu, allyl, Ph),[8] $[\alpha\text{-}T^{n+}W_{11}O_{39}(PhPO)_2]^{(8-n)-}$ (T = P^{5+}, Si^{4+}),[9] $[\alpha\text{-}PW_{11}O_{39}(PhPO)][PhPO(OH)]^{4-}$,[9] $[\gamma\text{-}SiW_{10}O_{36}(RPO)_2]^{4-}$ [R = H, Et, *n*Bu, *t*Bu, C_2H_4COOH, Ph],[10] and $[\gamma\text{-}H_2\{(SiW_{10}O_{36})[O{=}PCH_2(C_6H_4)_nCH_2P{=}O]\}_2]^{6-}$;[11] organogermanyl derivatives such as $[TW_{11}O_{39}\{GeCH_2CH_2X\}]^{n-}$ [T (isomer) = Si (α), Ge (α), Ga (a mixture of α and β); X = COOH, $COOCH_3$, $CONH_2$, CN; *n* = 5, 6];[2] and organosilyl derivatives such as $[\alpha\text{-}SiW_{11}O_{40}(SiR)_2]^{4-}$ [R = C_2H_5, $CH{=}CH_2$, $C_{10}H_{21}$, Ph, $NC(CH_2)_3$, C_3H_5],[12] $[\alpha_2\text{-}P_2W_{17}O_{61}\{O(SiR)_2\}]^{6-}$ {R = C_6H_5, 4-$[(C_2H_5O)_2P(=O)CH_2]$-C_6H_4, C_3H_6SH},[13,14] $[\gamma\text{-}PW_{10}O_{36}(t\text{BuSiOH})_2]^{3-}$,[15] $[\gamma\text{-}PW_{10}O_{36}(t\text{BuSiO})_2(SiMe_2)]^{3-}$,[15] $[\gamma\text{-}SiW_{10}O_{36}(RSiO)_4]^{4-}$ [R = Ph, $CH_2{=}C(CH_3)CO_2(CH_2)_3$],[16] $[\alpha\text{-}A\text{-}PW_9O_{34}(t\text{BuSiO})_3(SiR)]^{3-}$ [R = H, CH_3, Et, $CH{=}CH_2$, $CH_2\text{-}CH{=}CH_2$, $(CH_2)_4CH{=}CH_2$, $CH_2CH_2CH_2Cl$],[17,18] $[\alpha\text{-}A\text{-}TW_9O_{34}(R_2Si)_3]^{n-}$ (T = Si, P; R = Me, Ph; *n* = 3,4),[18] $[\alpha\text{-}A\text{-}PW_9O_{34}(t\text{BuSiOH})_3]^{3-}$,[18] $[\alpha\text{-}B\text{-}AsW_9O_{33}(t\text{BuSiOH})_3]^{3-}$,[18] $[\alpha\text{-}B\text{-}AsW_9O_{33}(t\text{BuSiO})_3(RSi)]^{3-}$,[18] $[\alpha\text{-}A\text{-}TW_9O_{34}(RSiO)_3(RSi)]^{n-}$ (T = Si, P; R = H, Me, C_2H_3, Et, *n*Bu; *n* = 3,4),[19,20] and $[\gamma\text{-}SiW_{10}O_{36}\{O(SiC_3H_6SH)_2\}]^{4-}$[21] have been reported. In particular, $[\alpha_2\text{-}P_2W_{17}O_{61}\{O(SiC_3H_6SH)_2\}]^{6-}$

[a] Department of Materials Science, Faculty of Science, Kanagawa University,
Tsuchiya 2946, Hiratsuka, Kanagawa 259-1293, Japan
Fax: +81-463-58-9684
E-mail: nomiya@kanagawa-u.ac.jp

Supporting information for this article is available on the WWW under http://www.eurjic.org or from the author.

and $[\gamma\text{-}SiW_{10}O_{36}\{O(SiC_3H_6SH)_2\}]^{4-}$ are intriguing examples of the use of organic moieties having an –SH group grafted to the lacunary sites of $[\alpha_2\text{-}P_2W_{17}O_{61}]^{10-}$ and $[\gamma\text{-}SiW_{10}O_{36}]^{8-}$ to derive new nanoscale hybrid systems in which covalent linkages between the polyoxometalate species and chlorobenzyl-functionalized polymer nanoparticles or gold nanoparticles are formed through the thiol groups. Although various types of complexes with organic groups have been prepared, the molecular structures of only a few complexes have been determined by X-ray crystallography. These include $[(\beta\text{-A-}PW_9O_{34})_2(PhSnOH)_3]^{12-}$,[5] $[\alpha\text{-}P_2W_{15}O_{59}(PhSn)_3]^{9-}$,[5] $[\beta\text{-}SiW_9O_{37}(PhSn)_3]^{7-}$,[6] $[(\alpha\text{-}SiW_9O_{34})_2(BuSnOH)_3]^{14-}$,[6] $[\alpha\text{-}PW_{11}O_{39}(PhPO)_2]^{3-}$,[9] $[\gamma\text{-}PW_{10}O_{36}(t\text{BuSiOH})_2]^{3-}$,[15] $[\alpha\text{-A-}PW_9O_{34}(t\text{BuSiO})_3(SiCH_2\text{-}CH{=}CH_2)]^{3-}$,[17] and $[\alpha\text{-A-}PW_9O_{34}(RSiO)_3(RSi)]^{3-}$ (R = C_2H_3, CH_3, C_2H_5).[18,20] In particular, X-ray crystal structure analyses of Dawson POM-based organic–inorganic hybrid compounds are crucial for polyoxoanion crystallography because of the difficulty in crystallizing them.

In this study, we report a series of Dawson-type POM-based organosilyl complexes containing $\{O[Si(CH_2)_3SH]_2\}$, $\{O[Si(CH_2)_3SCN]_2\}$, and $\{O(SiPh)_2\}$ groups, and the X-ray crystal structure analyses of $(Me_2NH_2)_5H[\alpha_2\text{-}P_2W_{17}O_{61}\{O[Si(CH_2)_3SH]_2\}]\cdot 6H_2O$ (Me_2NH_2-**1**), $(Me_2NH_2)_6[\alpha_2\text{-}P_2W_{17}O_{61}\{O[Si(CH_2)_3SCN]_2\}]\cdot 3H_2O$ (Me_2NH_2-**2**), and $(Me_2NH_2)_6[\alpha_2\text{-}P_2W_{17}O_{61}\{O(SiPh)_2\}]\cdot 4H_2O$ (Me_2NH_2-**3**). We describe their syntheses, characterization, and the molecular structures of compounds Me_2NH_2-(**1**–**3**) in complete detail.

Results and Discussion

Syntheses, Characterization, and Molecular Structures of a Series of the Dawson-Type POM-Based Organosilyl Compounds Me_2NH_2-(1–3)

The three compounds Me_2NH_2-(**1**–**3**) containing organosilyl groups were formed by direct reaction of the organosilyl precursors [$RSiX_3$; R = $HS(CH_2)_3$, $NCS(CH_2)_3$, and Ph; X = OMe, OEt, or Cl] with the mono-lacunary Dawson POM $[\alpha_2\text{-}P_2W_{17}O_{61}]^{10-}$ in an HCl/water/acetonitrile mixed solution or a water/acetonitrile mixed solution at room temperature in air, followed by crystallization from water in the dark. The formation of Me_2NH_2-(**1**–**3**) is given by the ionic balance shown in Equations (1), (2), and (3) in which the hydrolysis of Si–X bonds occurs upon addition of acid; the electrophilic organosilyl moieties then attack the lacunary surface sites of polyoxometalates.[13]

$$RSi(X)_3 + 3\ H_2O \rightarrow RSi(OH)_3 + 3\ XH \quad [R = HS(CH_2)_3,\ NCS(CH_2)_3;\ X = OMe,\ OEt] \quad (1)$$

$$[\alpha_2\text{-}P_2W_{17}O_{61}]^{10-} + 2\ RSi(OH)_3 + 4\ H^+ \rightarrow [\alpha_2\text{-}P_2W_{17}O_{61}\{O(SiR)_2\}]^{6-} + 5\ H_2O \quad (2)$$

$$[\alpha_2\text{-}P_2W_{17}O_{61}]^{10-} + 2\ PhSiCl_3 + H_2O \rightarrow [\alpha_2\text{-}P_2W_{17}O_{61}\{O(SiPh)_2\}]^{6-} + 2\ H^+ + 6\ Cl^- \quad (3)$$

The crystal structures of Me_2NH_2-**1** (Figure 1), Me_2NH_2-**2** (Figure 2), and Me_2NH_2-**3** (Figure 3) are composed of the mono-lacunary Dawson POM unit "$\alpha_2\text{-}P_2W_{17}O_{61}$" and the $\{O[Si(CH_2)_3SH]_2\}$, $\{O[Si(CH_2)_3SCN]_2\}$, and $\{O(SiPh)_2\}$ groups, respectively. Each silyl group is linked to two tungsten atoms located in two different positions of the mono-lacunary site through the bonding of four oxygen atoms O(2), O(3), O(6), and O(7) for Me_2NH_2-**1** and Me_2NH_2-**2**, which have C_1 symmetry for the polyanions **1** and **2**, and O(2), O(3), O(2A), and O(3A) for Me_2NH_2-**3**, which has C_s symmetry for polyanion **3**. Me_2NH_2-**1** and Me_2NH_2-**2** were found as a set of enantiomeric pairs in the unit cell, as shown in Figures 1 and 2, respectively. The lengths of the Si–O bonds coordi-

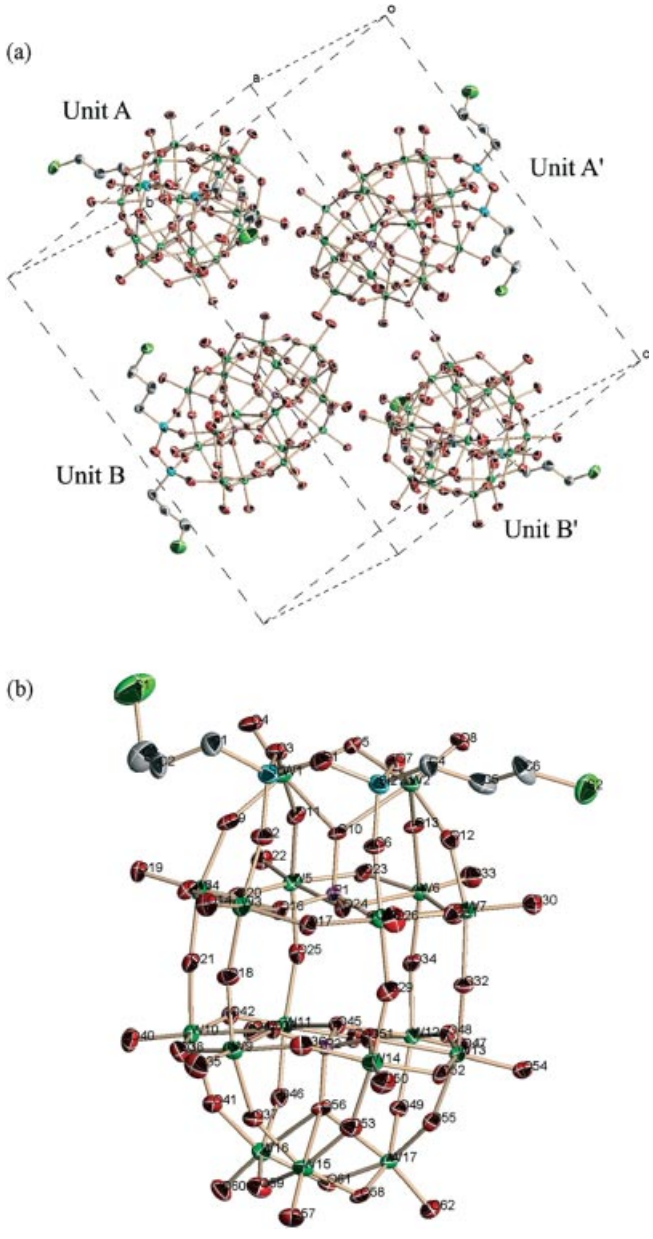

Figure 1. (a) The solid-state packing of Me_2NH_2-**1** (Z = 4) and (b) the molecular structure of Me_2NH_2-**1** with 50% probability ellipsoids. In (a), units (A, A′) and (B, B′) represent different sets of enantiomeric pairs. The molecular structure of unit A is depicted in (b).

nated to the four oxygen atoms in the lacunary site are in the range 1.611(12)–1.650(13) Å (average 1.64 Å) for Me_2NH_2-**1**, 1.608(12)–1.647(13) Å (1.63 Å) for Me_2NH_2-**2**, and 1.613(8)–1.651(8) Å (1.63 Å) for Me_2NH_2-**3** (see Tables 1, 2, and 3, respectively, and Tables S1–S3 in the Supporting Information). These values are similar to those of $[\gamma\text{-}PW_{10}O_{36}(t\text{BuSiOH})_2]^{3-}$ (1.62–1.70 Å)[15] and $[\alpha\text{-A-}PW_9O_{34}(t\text{BuSiO})_3(SiCH_2\text{-}CH{=}CH_2)]^{3-}$ (1.59–1.65 Å),[17] which have a similar tetrahedral environment of the silicon atom. On the other hand, the W–O lengths in the vacant site are in the range 1.873–1.919 Å [W(1)–O(3), W(2)–O(7), W(3)–O(2), and W(8)–O(6)] for Me_2NH_2-**1**, 1.889–1.912 Å [W(1)–O(3), W(2)–O(7), W(3)–O(2), and W(8)–O(6)] for Me_2NH_2-**2**, and 1.898–1.914 Å [W(1)–O(3) and W(2)–O(2)] for Me_2NH_2-**3**; these bonds are longer than those to the terminal oxygen in $[\alpha_2\text{-}P_2W_{17}O_{61}]^{10-}$ (ca. 1.7 Å).[22] Thus, the W–O lengths of the terminal oxygen in the vacant site of $[\alpha_2\text{-}P_2W_{17}O_{61}]^{10-}$ are stretched by the binding of the organosilyl groups. In contrast, the W–O lengths in the W_3 cap and the two W_6 belts, i.e. W–O_t (O_t: terminal oxygen), W–O_e (O_e: edge-sharing oxygen), W–O_c (W belt) (O_c: corner-sharing oxygen), and W–O_a (O_a: oxygen coordinated to the P atom) are in the normal range.[1b,22] The Si–O–Si bond angles for Me_2NH_2-(**1**–**3**) are 126.3(9)°, 124.7(8)°, and 127.4(7)°, respectively, which means they are much smaller than that of $[\alpha\text{-A-}PW_9O_{34}(t\text{BuSiO})_3(SiCH_2\text{–}CH{=}CH_2)]^{3-}$ (173.7°).[17]

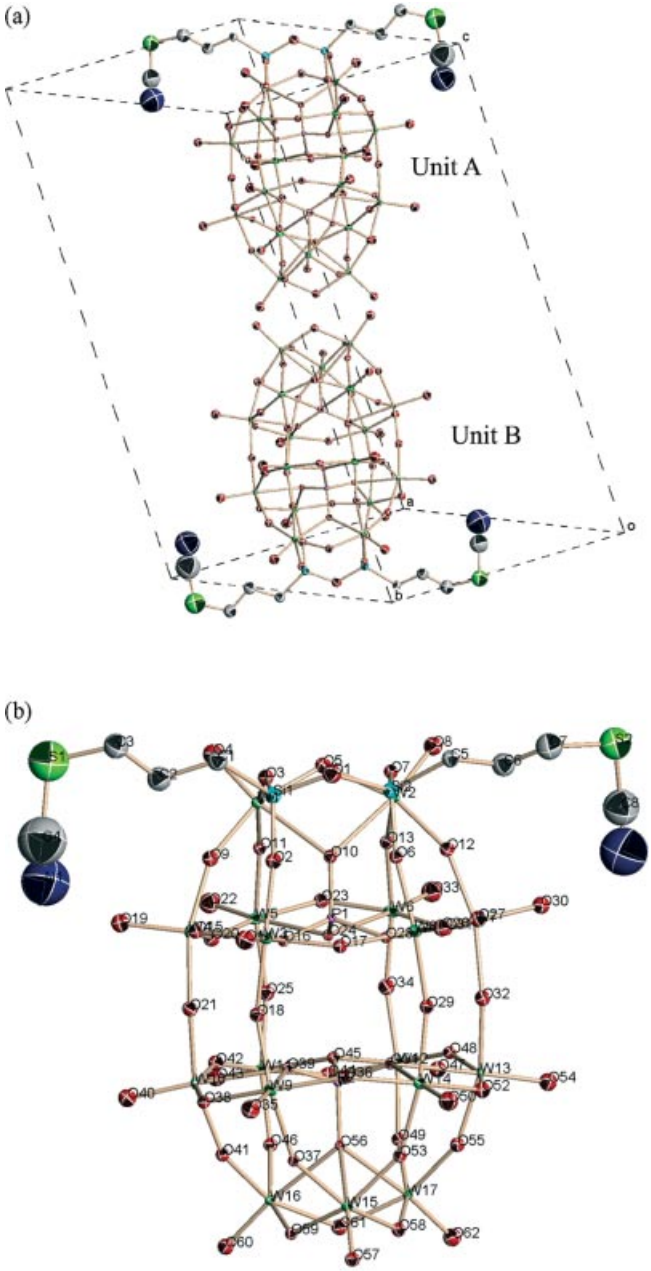

Figure 2. (a) The solid-state packing of Me_2NH_2-**2** (Z = 2) and (b) the molecular structure of Me_2NH_2-**2** with 50% probability ellipsoids. In (a), (A, B) represents an enantiomeric pair. The molecular structure of unit A is depicted in (b).

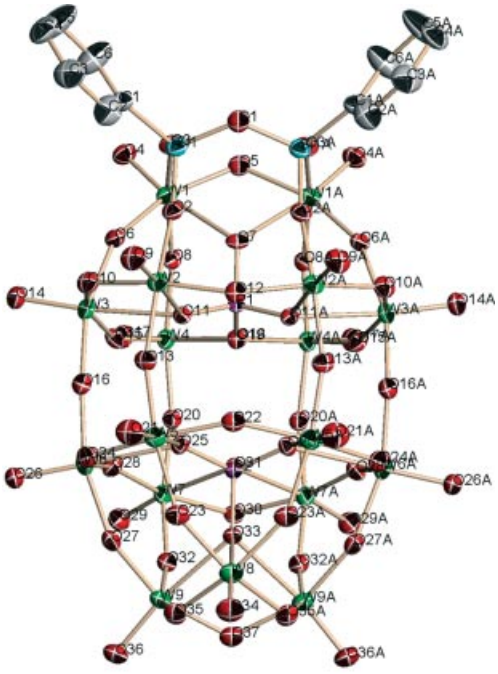

Figure 3. Molecular structure of Me_2NH_2-**3** with 50% probability ellipsoids.

With regard to the $\{O[Si(CH_2)_3SH]_2\}$ group of Me_2NH_2-**1**, it was noted that one of the two $HS(CH_2)_3Si$ moieties in this group is oriented in the equatorial direction while the other is oriented in the axial bonding direction. This unique configuration was found three times by X-ray crystallography. The Si–C bond lengths are in the range 1.86–1.87 Å and are slightly shorter than those of $[\gamma\text{-}PW_{10}O_{36}(t\text{Bu-SiOH})_2]^{3-}$ (1.94–1.97 Å).[15] The bond angles of the left $HS(CH_2)_3Si$ moiety [Si(1)–C(1)–C(2), C(1)–C(2)–C(3), and C(2)–C(3)–S(1)] are larger than those of the right moiety [Si(2)–C(4)–C(5), C(4)–C(5)–C(6), C(5)–C(6)–S(2)], as shown in Table 1. In the case of the $\{O[Si(CH_2)_3SCN]_2\}$ group of Me_2NH_2-**2**, the two $NCS(CH_2)_3Si$ moieties are oriented in a *syn* fashion. This configuration was also found twice by X-ray crystallography. The Si–C bond lengths are in the range 1.84–1.89 Å and are similar to those of Me_2NH_2-**1**. The S(1)–C(4) distance [1.97(6) Å] is somewhat longer than that of S(2)–C(8) [1.71(4) Å]. The bond angles

Table 1. Selected bond lengths [Å] and angles [°] for Me_2NH_2-**1** around the $\{O[Si(CH_2)_3SH]_2\}$ group.

Bond lengths			
Si(1)–O(1)	1.637(15)	C(2)–C(3)	1.48(3)
Si(1)–O(2)	1.632(12)	C(3)–S(1)	1.81(3)
Si(1)–O(3)	1.649(14)	C(4)–C(5)	1.58(3)
Si(1)–C(1)	1.86(2)	C(5)–C(6)	1.52(3)
Si(2)–O(1)	1.631(14)	C(6)–S(2)	1.85(2)
Si(2)–O(6)	1.611(12)	W(1)–O(3)	1.919(13)
Si(2)–O(7)	1.650(13)	W(2)–O(7)	1.908(12)
Si(2)–C(4)	1.869(19)	W(3)–O(2)	1.873(11)
C(1)–C(2)	1.55(3)	W(8)–O(6)	1.887(11)
Bond angles			
O(1)–Si(1)–O(2)	106.8(7)	Si(1)–O(1)–Si(2)	126.3(9)
O(2)–Si(1)–O(3)	109.8(7)	Si(1)–O(2)–W(3)	168.2(8)
O(3)–Si(1)–O(1)	106.8(7)	Si(1)–O(3)–W(1)	142.6(7)
O(1)–Si(1)–C(1)	109.9(8)	Si(2)–O(6)–W(8)	168.1(8)
O(2)–Si(1)–C(1)	110.2(8)	Si(2)–O(7)–W(2)	143.2(7)
O(3)–Si(1)–C(1)	113.0(9)	Si(1)–C(1)–C(2)	114.2(14)
O(1)–Si(2)–O(6)	107.4(7)	C(1)–C(2)–C(3)	118.2(19)
O(6)–Si(2)–O(7)	110.7(7)	C(2)–C(3)–S(1)	114.9(18)
O(7)–Si(2)–O(1)	106.6(7)	Si(2)–C(4)–C(5)	105.9(13)
O(1)–Si(2)–C(4)	113.5(8)	C(4)–C(5)–C(6)	107.9(17)
O(6)–Si(2)–C(4)	108.2(8)	C(5)–C(6)–S(2)	107.0(15)
O(7)–Si(2)–C(4)	110.4(8)		

Table 2. Selected bond lengths [Å] and angles [°] for Me_2NH_2-**2** around the $\{O[Si(CH_2)_3SCN]_2\}$ group.

Bond lengths			
Si(1)–O(1)	1.632(13)	S(1)–C(4)	1.97(6)
Si(1)–O(2)	1.627(12)	N(1)–C(4)	1.15(6)
Si(1)–O(3)	1.608(12)	C(5)–C(6)	1.48(3)
Si(1)–C(1)	1.84(2)	C(6)–C(7)	1.45(3)
Si(2)–O(1)	1.647(13)	C(7)–S(2)	1.77(3)
Si(2)–O(6)	1.630(11)	S(2)–C(8)	1.71(4)
Si(2)–O(7)	1.629(12)	C(8)–N(2)	1.10(5)
Si(2)–C(5)	1.890(18)	W(1)–O(3)	1.905(11)
C(1)–C(2)	1.56(3)	W(2)–O(7)	1.889(10)
C(2)–C(3)	1.50(3)	W(3)–O(2)	1.912(11)
C(3)–S(1)	1.77(3)	W(8)–O(6)	1.893(11)
Bond angles			
O(1)–Si(1)–O(2)	106.2(7)	Si(1)–O(3)–W(1)	145.3(7)
O(2)–Si(1)–O(3)	111.2(6)	Si(2)–O(6)–W(8)	169.0(7)
O(3)–Si(1)–O(1)	108.8(7)	Si(2)–O(7)–W(2)	143.9(7)
O(1)–Si(1)–C(1)	110.3(8)	Si(1)–C(1)–C(2)	113.7(13)
O(2)–Si(1)–C(1)	115.1(8)	C(1)–C(2)–C(3)	111.1(17)
O(3)–Si(1)–C(1)	105.1(8)	C(2)–C(3)–S(1)	114.2(16)
O(1)–Si(2)–O(6)	107.9(6)	C(3)–S(1)–C(4)	107(2)
O(6)–Si(2)–O(7)	108.1(6)	S(1)–C(4)–N(1)	150(6)
O(7)–Si(2)–O(1)	108.1(7)	Si(2)–C(5)–C(6)	113.9(13)
O(1)–Si(2)–C(5)	112.4(7)	C(5)–C(6)–C(7)	112.1(18)
O(6)–Si(2)–C(5)	110.0(7)	C(6)–C(7)–S(2)	119.1(18)
O(7)–Si(2)–C(5)	110.3(7)	C(7)–S(2)–C(8)	101.6(16)
Si(1)–O(1)–Si(2)	124.7(8)	S(2)–C(8)–N(2)	166(4)
Si(1)–O(2)–W(3)	172.9(8)		

of the left $NCS(CH_2)_3Si$ moiety [Si(1)–C(1)–C(2) and C(1)–C(2)–C(3)] are similar to those of the right moiety [Si(2)–C(5)–C(6) and C(5)–C(6)–C(7)]; however, the C(2)–C(3)–S(1), C(3)–S(1)–C(4), and particularly, S(1)–C(4)–N(1) bond angles are quite different from those of C(6)–C(7)–S(2), C(7)–S(2)–C(8), and S(2)–C(8)–N(2), respectively, as shown in Table 2. For the $\{O(SiPh)_2\}$ group of Me_2NH_2-**3**, the Si–C bond length is 1.85 Å, which is similar to those of Me_2NH_2-**1** and Me_2NH_2-**2**, as shown in Table 3.

Table 3. Selected bond lengths [Å] and angles [°] for Me_2NH_2-**3** around the $\{O(SiPh)_2\}$ group.

Bond lengths			
Si(1)–O(1)	1.634(6)	C(3)–C(4)	1.40(2)
Si(1)–O(2)	1.613(8)	C(4)–C(5)	1.37(2)
Si(1)–O(3)	1.651(8)	C(5)–C(6)	1.38(2)
Si(1)–C(1)	1.847(11)	C(6)–C(1)	1.395(19)
Si(1A)–O(1)	1.634(6)	W(1)–O(3)	1.914(7)
C(1)–C(2)	1.394(18)	W(2)–O(2)	1.898(8)
C(2)–C(3)	1.42(2)		
Bond angles			
O(1)–Si(1)–O(2)	108.2(5)	C(1)–C(2)–C(3)	119.9(14)
O(2)–Si(1)–O(3)	111.5(4)	C(2)–C(3)–C(4)	119.4(14)
O(3)–Si(1)–O(1)	106.2(5)	C(3)–C(4)–C(5)	119.7(13)
O(1)–Si(1)–C(1)	108.4(5)	C(4)–C(5)–C(6)	120.7(16)
O(2)–Si(1)–C(1)	111.8(5)	C(5)–C(6)–C(1)	121.5(15)
O(3)–Si(1)–C(1)	110.5(5)	Si(1)–O(1)–Si(1A)	127.4(7)
C(2)–C(1)–C(6)	118.5(12)	Si(1)–O(2)–W(2)	170.7(5)
C(2)–C(1)–Si(1)	118.0(10)	Si(1)–O(3)–W(1)	139.9(5)
C(6)–C(1)–Si(1)	123.5(10)		

The bond valence sums (BVS) for Me_2NH_2-(**1**–**3**),[23] calculated on the basis of the observed bond lengths, are in the range 5.950–6.232 (average 6.12), 6.017–6.359 (6.18), and 6.105–6.289 (6.16) for the 17 W atoms, respectively, those of the two P atoms are in the range 4.833–4.877 (average 4.86), 4.908–5.127 (5.02), and 4.901–4.933 (4.92), respectively, and those of the 62 O atoms are in the range 1.618–2.166 (average 1.90), 1.635–2.172 (1.96), and 1.717–2.174 (1.95), respectively. These values correspond reasonably well to the formal valences W^{6+}, P^{5+}, and O^{2-}, respectively (see Tables S4–S6 in the Supporting Information).

The crystal structures of Me_2NH_2-(**1**–**3**) are consistent with the elemental analyses, TG/DTA data, and FTIR, solution NMR (^1H, ^{13}C, and ^{31}P), and solid-state ^{13}C NMR spectra. The elemental analyses had to be performed for compounds Me_2NH_2-(**1**–**3**) after drying them at room temperature at 10^{-3}–10^{-4} Torr overnight before the results were consistent with the compositions $(Me_2NH_2)_5H[\alpha_2$-$P_2W_{17}O_{61}\{O[Si(CH_2)_3SH]_2\}]$, $(Me_2NH_2)_6[\alpha_2$-$P_2W_{17}O_{61}$-$\{O[Si(CH_2)_3SCN]_2\}]$, and $(Me_2NH_2)_6[\alpha_2$-$P_2W_{17}O_{61}$-$\{O(SiPh)_2\}]$, respectively. The TG/DTA measurements performed under atmospheric conditions showed a weight loss of 2.38%, 1.27%, and 1.62%, with an endothermic point at 67, 37, and 86 °C, respectively; these values correspond to the presence of 6, 3, and 4 water molecules, respectively, due to both the intrinsic water of hydration and the water adsorbed from the atmosphere. Thus, the number of hydrated water molecules in compounds Me_2NH_2-(**1**–**3**) is 6, 3, and 4, respectively.

The FTIR spectra of compounds Me_2NH_2-(**1**–**3**) measured as a KBr disk are shown in Figure 4. The spectral patterns of these compounds are similar to those of $[\alpha_2$-$P_2W_{17}O_{61}]^{10-}$ (1086, 1054, 1016, 940, 885, 811, 741, 601, 527, and 467 cm^{-1}) rather than those of $[\alpha$-$P_2W_{18}O_{62}]^{6-}$ (1088, 1040, 956, 925, and 713 cm^{-1}). The additional bands observed at 2566 and 2154 cm^{-1} in the case of compounds

Me_2NH_2-**1** and Me_2NH_2-**2** were assigned to the SH and SCN moieties, respectively.[24]

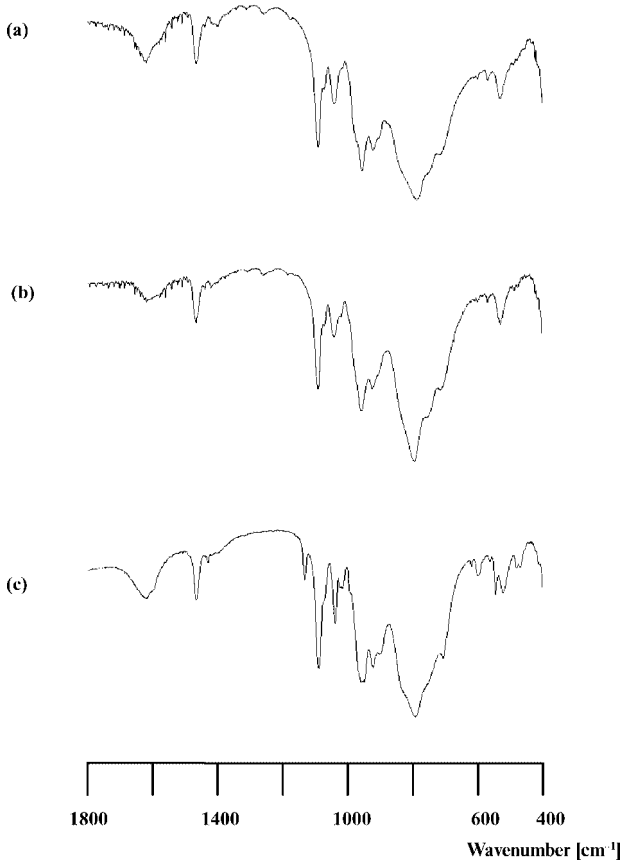

Figure 4. FTIR spectra, measured as KBr disks, in the polyoxoanion region (1800–400 cm^{-1}) of (a) Me_2NH_2-**1**, (b) Me_2NH_2-**2**, and (c) Me_2NH_2-**3**.

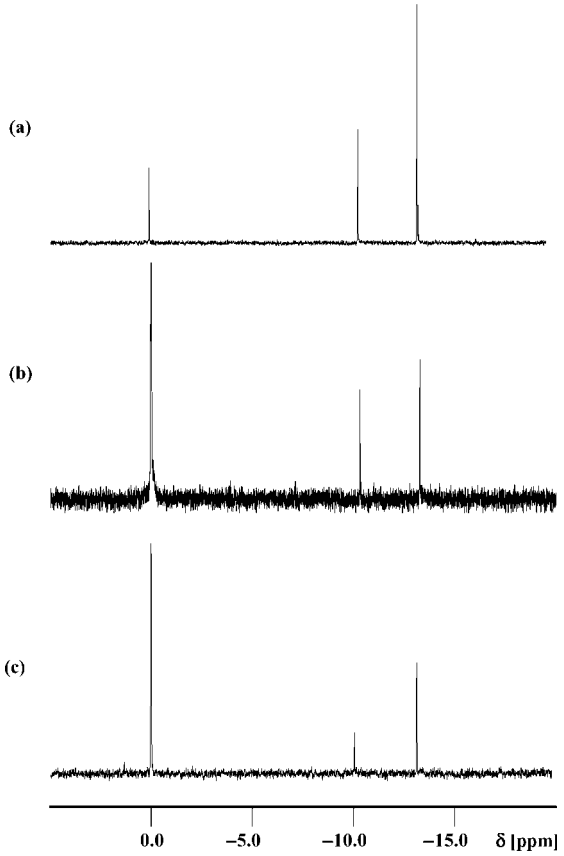

Figure 5. ^{31}P NMR spectra in D_2O of (a) Me_2NH_2-**1**, (b) Me_2NH_2-**2**, and (c) Me_2NH_2-**3**.

The ^{31}P NMR spectra of compounds Me_2NH_2-(**1**–**3**) in D_2O at about 25 °C show a clear two-line spectrum at δ = –10.52 and –13.50 ppm, δ = –10.33 and –13.28 ppm, and δ = –10.21 and –13.29 ppm, respectively, thereby confirming their purity and homogeneity (see Figure 5). The downfield resonance was assigned to the phosphorus closest to the organosilyl sites and the upfield resonance to the phosphorus closer to the W_3 cap.

The ^1H NMR spectra of Me_2NH_2-**1** and Me_2NH_2-**2** in D_2O at about 25 °C show signals at δ = 0.93–1.03, 1.95–1.96, and 2.72–2.77 ppm and δ = 1.04–1.10, 2.18–2.21, and 3.28–3.31 ppm, respectively, arising from the two $–(CH_2)_3–$ groups in the $\{O[Si(CH_2)_3SH]_2\}$ and $\{O[Si(CH_2)_3SCN]_2\}$ groups, respectively (Table 4). For Me_2NH_2-**3**, ^1H signals assigned to the two phenyl groups in the $\{O(SiPh)_2\}$ moiety are observed at δ = 7.53–7.94 ppm. The ^{13}C NMR spectra of Me_2NH_2-**1** and Me_2NH_2-**2** in D_2O at about 25 °C show signals at δ = 13.2, 29.1, and 29.9 ppm and δ = 12.8, 26.1, and 38.4 ppm, respectively, which can also be assigned to the two $–(CH_2)_3–$ groups in the $\{O[Si(CH_2)_3SH]_2\}$ and $\{O[Si(CH_2)_3SCN]_2\}$ groups, respectively (Table 4). The ^{13}C NMR spectrum of Me_2NH_2-**2** also shows a signal at δ = 117.9 ppm due to the SCN group. For Me_2NH_2-**3**, ^{13}C signals due to the two phenyl groups are observed at δ = 131.1–137.3 ppm. In aqueous solution, the two $HS(CH_2)_3$-Si moieties in the $\{O[Si(CH_2)_3SH]_2\}$ group and the two $NCS(CH_2)_3Si$ moieties in the $\{O[Si(CH_2)_3SCN]_2\}$ group cannot be distinguished by ^1H and ^{13}C NMR spectroscopy.

Table 4. Solution ^1H and ^{13}C NMR spectroscopic data for compounds Me_2NH_2-(**1**–**3**).

	^1H [δ, ppm]	^{13}C [δ, ppm]
Me_2NH_2-**1**	0.93–1.03 (H1)	13.2 (C1)
	1.95–1.96 (H2)	29.1 (C3)
	2.72–2.77 (H3)	29.9 (C2)
	2.80 (Me_2NH_2)	37.6 (Me_2NH_2)
Me_2NH_2-**2**	1.04–1.10 (H1)	12.8 (C1)
	2.18–2.21(H2)	26.1 (C2)
	3.28–3.31 (H3)	38.4 (C3)
	2.81 (Me_2NH_2)	37.4 (Me_2NH_2)
		117.9 (S*C*N)
Me_2NH_2-**3**	7.53–7.94 (Ph)	131.1–137.3 (Ph)
	2.76 (Me_2NH_2)	37.6 (Me_2NH_2)

In order to determine the configuration of the two $HS(CH_2)_3Si$ moieties in the $\{O[Si(CH_2)_3SH]_2\}$ group and the two $NCS(CH_2)_3Si$ moieties in the $\{O[Si(CH_2)_3SCN]_2\}$ group in the bulk samples, we measured the solid-state ^{13}C

NMR spectra for Me_2NH_2-**1** and Me_2NH_2-**2** (see Figure 6). In the spectrum of Me_2NH_2-**1**, C1 appears as two signals at δ = 12.7 ppm and 14.3 ppm; this is because of the different configuration, i.e. the equatorial and axial bonding of each of the two $HS(CH_2)_3Si$ moieties in the $\{O[Si(CH_2)_3SH]_2\}$ group. The C2 and C3 signals could not be identified owing to broadening of the signals. For Me_2NH_2-**2**, a broadening of the C1 signal is observed because of the somewhat different configurations of the two $NCS(CH_2)_3Si$ moieties, which are in a *syn* fashion in the $\{O[Si(CH_2)_3SCN]_2\}$ group (Scheme 1). The C3 signal could not be distinguished because of overlap with the Me_2NH_2 signal. These results are consistent with the X-ray structures and suggest that the configuration of the organosilyl groups of Me_2NH_2-**1** and Me_2NH_2-**2** observed by X-ray crystallography represents the solid structure of the bulk samples; these structures are not maintained in aqueous solution because of the mobility and/or flexibility of organosilyl groups that have straight-chain carbon structures.

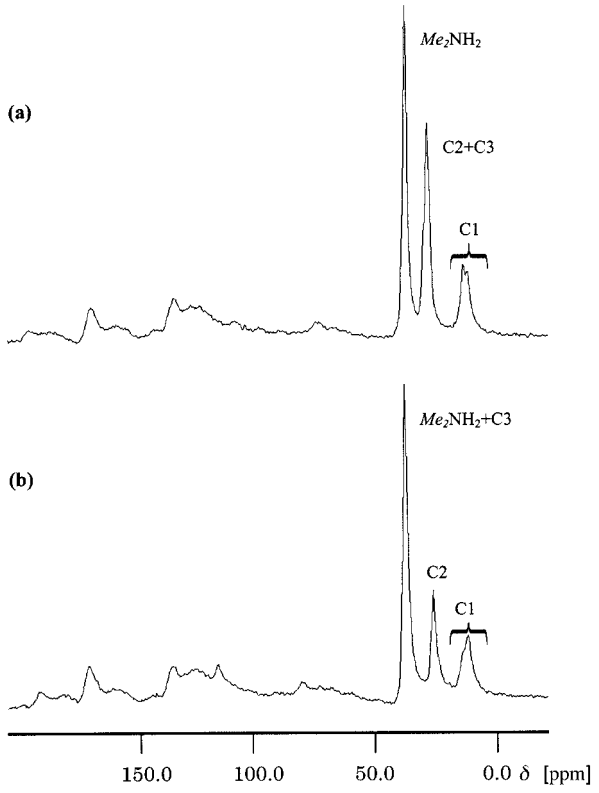

Figure 6. Solid-state ^{13}C NMR spectra of (a) Me_2NH_2-**1** and (b) Me_2NH_2-**2**.

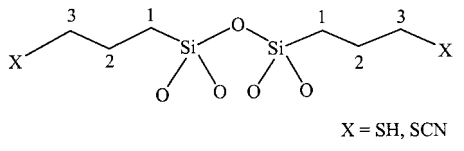

Scheme 1. Drawings of the $\{O[Si(CH_2)_3SH]_2\}$ and $\{O[Si(CH_2)_3SCN]_2\}$ groups.

Conclusions

A series of organosilyl complexes with the Dawson mono-lacunary phosphotungstate $[\alpha_2\text{-}P_2W_{17}O_{61}]^{10-}$ is presented. We have successfully obtained single crystals of the water-soluble dimethylammonium salts $(Me_2NH_2)_5H[\alpha_2\text{-}P_2W_{17}O_{61}\{O[Si(CH_2)_3SH]_2\}]\cdot 6H_2O$, $(Me_2NH_2)_6[\alpha_2\text{-}P_2W_{17}O_{61}\{O[Si(CH_2)_3SCN]_2\}]\cdot 3H_2O$, and $(Me_2NH_2)_6[\alpha_2\text{-}P_2W_{17}O_{61}\{O(SiPh)_2\}]\cdot 4H_2O$ by treating the organosilyl precursors $HS(CH_2)_3Si(OMe)_3$, $NCS(CH_2)_3Si(OEt)_3$, and $PhSiCl_3$, respectively, with the mono-lacunary polyoxoanion. The characterization of compounds Me_2NH_2-(**1**–**3**) has been accomplished by X-ray structure analyses, elemental analysis, TG/DTA, and FTIR and solution (^1H, ^{13}C, and ^{31}P) and solid-state ^{13}C NMR spectroscopy. The crystal structures of Me_2NH_2-(**1**–**3**) reveal that each silyl group is linked to two tungsten atoms that are located in two different positions of the mono-lacunary site by the bonding of four oxygen atoms for Me_2NH_2-**1** and Me_2NH_2-**2** with C_1 symmetry and Me_2NH_2-**3** with the C_s symmetry. The organosilyl groups with straight-chain carbon structures bound to the vacant site of $[\alpha_2\text{-}P_2W_{17}O_{61}]^{10-}$ have unique configurations, i.e. equatorial and axial bonding for each of the two $HS(CH_2)_3Si$ moieties in the $\{O[Si(CH_2)_3SH]_2\}$ group of Me_2NH_2-**1** and the two $NCS(CH_2)_3Si$ moieties oriented in a *syn* fashion in the $\{O[Si(CH_2)_3SCN]_2\}$ group of Me_2NH_2-**2**. Although these unique configurations are not maintained in aqueous solution, the crystal structures of these compounds represent the solid structures of the bulk samples. To the best of our knowledge, the X-ray crystal structures of compounds Me_2NH_2-(**1**–**3**) are the first examples of the molecular structures of Dawson-type polyoxometalate-based organosilyl complexes. Preliminary experiments show that it is possible to graft these polyoxometalates onto polymers.

Experimental Section

Materials: $K_{10}[\alpha_2\text{-}P_2W_{17}O_{61}]\cdot 19H_2O$ was prepared as described in the literature.[25] The number of solvated water molecules was determined by TG/DTA analysis. All reagents and solvents (acetonitrile, ethanol, methanol, and diethyl ether) were obtained from commercial sources and used as received. $HS(CH_2)_3Si(OMe)_3$, $NCS(CH_2)_3Si(OEt)_3$, and $PhSiCl_3$ were obtained from Azmax.

Instrumentation/Analytical Procedures: Elemental analyses were carried out with a Perkin–Elmer 2400 CHNS Elemental Analyzer II (Kanagawa University) and Mikroanalytisches Labor Pascher (Remagen, Germany). The samples were dried at room temperature at 10^{-3}–10^{-4} Torr overnight before analysis. IR spectra were recorded with a Jasco 4100 FT-IR spectrometer in KBr disks at room temperature. Thermogravimetric (TG) and differential thermal analyses (DTA) data were acquired using a Rigaku Thermo Plus 2 series TG/DTA TG 8120 instrument. TG/DTA measurements were performed in air with a temperature ramp of 4 °C per minute between 20 and 500 °C. The ^1H (399.65 MHz), $^{13}C\{^1H\}$ (100.40 MHz), and $^{31}P\{^1H\}$ NMR (161.70 MHz) spectra in solution were recorded in 5-mm outer diameter tubes with a JEOL JNM-EX 400 FT-NMR spectrometer equipped with a JEOL EX-400 data-processing system. ^1H and $^{13}C\{^1H\}$ NMR spectra of the

complexes were measured in D_2O solution with reference to internal DSS or TSP [sodium 2,2,3,3-[D_4]3-(trimethylsilyl)propionate]. Chemical shifts are reported as positive for resonances downfield of DSS or TSP (δ = 0 ppm). The $^{31}P\{^1H\}$ NMR spectra were referenced to an external standard of 25% H_3PO_4 in H_2O in a sealed capillary. Chemical shifts are reported as negative on the δ scale with resonances upfield of H_3PO_4 (δ = 0 ppm). Solid-state ^{13}C NMR spectra were recorded at 300 MHz with a JEOL JNM-ECP 300 FT-NMR spectrometer equipped with a JEOL ECP-300 data-processing system. The chemical shifts are referenced to $C_6(CH_3)_6$ and are reported to be positive on the δ scale with resonances upfield of the methyl group of $C_6(CH_3)_6$ (δ = 17.4 ppm).

Synthesis and Crystallization of $(Me_2NH_2)_5H[\alpha_2$-$P_2W_{17}O_{61}$-$\{O[Si(CH_2)_3SH]_2\}]\cdot 6H_2O$ (Me_2NH_2-1): $K_{10}[\alpha_2$-$P_2W_{17}O_{61}]\cdot 19H_2O$ (5.00 g, 1.00 mmol) was added to a colorless clear solution of $HS(CH_2)_3Si(OMe)_3$ (380 μL, 2.00 mmol [d = 1.056]) dissolved in a mixture of water (50 mL) and CH_3CN (150 mL), and the pH was adjusted to 1.8 with 1 M aqueous HCl. After stirring for 30 min, the solution was evaporated to a volume of about 30 mL on a rotary evaporator at 30 °C. Me_2NH_2Cl (5.5 g, 67.5 mmol) was then added to the resulting pale-yellow clear solution. Hereafter, the experiments were performed in the dark because the precipitate is sensitive to light. A yellow-white precipitate was formed, which was collected on a membrane filter (JG, 0.2 μm), and washed with methanol (3 × 30 mL) and diethyl ether (3 × 30 mL). At this stage, the crude dimethylammonium salt was obtained in 4.15 g yield. A portion of this crude product (0.5 g) was dissolved in aqueous HCl (4 mL of 6 M solution) in a water bath at about 60 °C. The clear yellow solution was then slowly evaporated at room temperature in the dark. After 2 d, clear yellow granular crystals were formed. The crystals were obtained in 14.8% (0.070 g scale) yield based on $(Me_2NH_2)_5H[\alpha_2$-$P_2W_{17}O_{61}\{O[Si(CH_2)_3SH]_2\}]\cdot 6H_2O$. Me_2NH_2-**1** is very soluble in acetonitrile and dimethyl sulfoxide, soluble in water, and insoluble in methanol, ethanol, acetone, ethyl acetate, dichloromethane, and diethyl ether. The solid sample gradually changes to blue upon exposure to light and is slightly hygroscopic. $(Me_2NH_2)_5H[\alpha_2$-$P_2W_{17}O_{61}\{O[Si(CH_2)_3SH]_2\}]\cdot xH_2O$ (x = 0), $C_{16}H_{55}N_5O_{62}P_2W_{17}S_2Si_2$ (4617.1): calcd. C 4.16, H 1.20, N 1.52, P 1.34, S 1.39, Si 1.22, W 67.69; found C 3.52 (3.97) [3.88], H 1.14 (1.24), N 1.35 (1.39), P 1.30, S 1.29, Si 1.32, W 67.6. The values in round and square brackets are the 2nd and 3rd data, respectively, which were measured at Kanagawa University. A weight loss of 2.21% was observed during the course of overnight drying at room temperature at 10^{-3}–10^{-4} Torr before the analyses, which suggests the presence of between five and six weakly solvated or adsorbed water molecules. TG/DTA under atmospheric conditions: a weight loss of 2.38% with an endothermic point at 67 °C was observed below 137 °C; calcd. 2.29% for x = 6 in $(Me_2NH_2)_5H[\alpha_2$-$P_2W_{17}O_{61}\{O[Si(CH_2)_3SH]_2\}]\cdot xH_2O$. IR (KBr disk): $\tilde{\nu}$ = 2571 (m) [SH], 1623 (s), 1507 (w), 1465 (s), 1437 (w), 1412 (w), 1399 (w), 1374 (w), 1362 (w), 1339 (w), 1308 (w), 1254 (w), 1173 (w), 1088 (vs), 1069 (w), 1038 (s), 953 (s), 920 (m), 783 (vs, br.), 714 (w), 596 (w), 565 (w), 526 (m), 486 (w), 476 (w), 431 (w), 419 (w) cm^{-1}. ^1H NMR (22.6 °C, D_2O): δ = 0.93–1.03 (H1), 1.95–1.96 (H2), 2.72–2.77 (H3), 2.80 (Me_2NH_2) ppm. ^{13}C NMR (25.4 °C, D_2O): δ = 13.2 (C1), 29.1 (C3), 29.9 (C2), 37.6 (Me_2NH_2) ppm. ^{31}P NMR (23.3 °C, D_2O): δ = –10.52, –13.50 ppm. The ^{183}W NMR measurement in D_2O was unsuccessful because the concentration of Me_2NH_2-**1** in aqueous solution was insufficient. Solid-state ^{13}C NMR: δ = 12.7 (C1), 14.3 (C1), 28.8 (C2, C3), 37.8 (Me_2NH_2) ppm.

Synthesis and Crystallization of $(Me_2NH_2)_6[\alpha_2$-$P_2W_{17}O_{61}$-$\{O[Si(CH_2)_3SCN]_2\}]\cdot 3H_2O$ (Me_2NH_2-2): $K_{10}[\alpha_2$-$P_2W_{17}O_{61}]\cdot 19H_2O$ (5.00 g, 1.00 mmol) was added to a colorless clear solution of $NCS(CH_2)_3Si(OEt)_3$ (767 μL, 3.00 mmol [d = 1.03]) dissolved in a mixture of water (50 mL) and CH_3CN (150 mL), and the pH was adjusted to 1.8 with 1 M aqueous HCl. After stirring for 30 min, the solution was evaporated to a volume of about 30 mL on a rotary evaporator at 30 °C. Me_2NH_2Cl (5.0 g, 61.3 mmol) was then added to this pale-yellow clear solution. Hereafter, the experiments were performed in the dark because the precipitate is sensitive to light. A yellow-white precipitate was formed, which was collected on a membrane filter (JG, 0.2 μm) and washed with ethanol (3 × 30 mL) and diethyl ether (3 × 30 mL). At this stage the crude dimethylammonium salt was obtained in 4.31 g yield. A portion of this crude product (0.5 g) was dissolved in water (9.5 mL) in a water bath at about 80 °C and then cooled to about 25 °C. After 1 d, the crude crystalline precipitate was removed by filtering through a folded filter paper (Watman #2). The resulting clear pale-yellow solution was slowly evaporated at room temperature in the dark. After 6 d, pale-yellow plate crystals were formed. The crystals were obtained in 17.8% (0.085 g scale) yield based on $(Me_2NH_2)_6[\alpha_2$-$P_2W_{17}O_{61}\{O[Si(CH_2)_3SCN]_2\}]\cdot 3H_2O$. Me_2NH_2-**2** is soluble in water, dimethyl sulfoxide, and acetonitrile, while it is insoluble in methanol, ethanol, ethyl acetate, and diethyl ether. The solid sample gradually became blue upon exposure to light and is slightly hygroscopic. $(Me_2NH_2)_6[\alpha_2$-$P_2W_{17}O_{61}\{O[Si(CH_2)_3SCN]_2\}]\cdot xH_2O$ (x = 0), $C_{20}H_{60}N_8O_{62}P_2W_{17}Si_2S_2$ (4712.2): calcd. C 5.10, H 1.28, N 2.38, P 1.31, S 1.36, Si 1.19, W 66.32; found C 5.03, H 1.27, N 2.40, P 1.29, S 1.27, Si 1.33, W 66.2. A weight loss of 1.55% was observed during the course of overnight drying at room temperature and 10^{-3}–10^{-4} Torr before the analyses, which suggests the presence of between four and five weakly solvated or adsorbed water molecules. TG/DTA under atmospheric conditions: a weight loss of 1.27% with an endothermic point at 37 °C was observed below 140 °C; calcd. 1.13% for x = 3 in $(Me_2NH_2)_6[\alpha_2$-$P_2W_{17}O_{61}\{O(SiC_3H_6SCN)_2\}]\cdot xH_2O$. The number of solvated or adsorbed water molecules determined by TG/DTA was slightly different from that measured by Pascher (Germany) because the TG/DTA data are dependent on the conditions before analysis. Here, we used three water molecules for the X-ray crystal analysis. IR (KBr disk): $\tilde{\nu}$ = 2154 (m) [SCN], 1616 (m), 1465 (m), 1437 (w), 1418 (w), 1305 (w), 1257 (w), 1182 (w), 1089 (vs), 1069 (w), 1038 (m), 955 (vs), 922 (w), 794 (vs, br.), 710 (w), 669 (w), 597 (w), 584 (w), 566 (w), 526 (m), 484 (w), 472 (w) cm^{-1}. ^1H NMR (24.5 °C, D_2O): δ = 1.04–1.10 (H1), 2.18–2.21 (H2), 3.28–3.31 (H3), 2.81 (Me_2NH_2) ppm. ^{13}C NMR (25.5 °C, D_2O): δ = 12.8 (C1), 26.1(C2), 38.4 (C3), 37.4 (Me_2NH_2), 117.9 (S*C*N) ppm. ^{31}P NMR (23.6 °C, D_2O): δ = –10.33, –13.28 ppm. The ^{183}W NMR measurement in D_2O was unsuccessful because the concentration of Me_2NH_2-**2** in aqueous solution was insufficient. Solid-state ^{13}C NMR: δ = 12.31 (sh) (C1), 26.41 (C2), 38.16 (Me_2NH_2, C3) ppm.

Synthesis and Crystallization of $(Me_2NH_2)_6[\alpha_2$-$P_2W_{17}O_{61}\{O$-$(SiPh)_2\}]\cdot 4H_2O$ (Me_2NH_2-3): Me_2NH_2-**3** was synthesized by a modification of the reported method.[13] $K_{10}[\alpha_2$-$P_2W_{17}O_{61}]\cdot 19H_2O$ (5.00 g, 1.00 mmol) was added to a colorless clear solution of $C_6H_5SiCl_3$ (325 μL, 2.00 mmol [d = 1.28]) dissolved in a mixture of water (50 mL) and CH_3CN (250 mL) and stirred for 1 h. The solution was evaporated to about 40 mL on a rotary evaporator at 30 °C. The pale-yellow suspension was filtered through a membrane filter (JG, 0.2 μm), and the resulting pale-yellow clear filtrate was re-evaporated to about 35 mL in a water bath at about 80 °C. After filtration through a membrane filter (JG, 0.2 μm), Me_2NH_2Cl (5.5 g, 67.5 mmol) was added to the pale-yellow filtrate. Hereafter, the experiments were performed in the dark because the powder formed is sensitive to light. A white precipitate and yellow oil were formed. After stirring in the dark for 10 min in a water bath at

about 80 °C, the solution was cooled to room temperature. A yellow-white precipitate was formed, which was collected on a membrane filter (JG, 0.2 μm), and washed with ethanol (3 × 10 mL) and diethyl ether (3 × 30 mL). At this stage the crude dimethylammonium salt was obtained in 3.62 g yield. A portion of this crude product (2.00 g) was dissolved in water (50 mL) in a water bath at 80 °C and filtered through a folded filter paper while the solution was hot. The pale-yellow clear filtrate was slowly evaporated at room temperature in the dark. After 3 d, yellow granular crystals were formed. The crystals were obtained in 37.0% (0.74 g scale) yield based on $(Me_2NH_2)_6[\alpha_2\text{-}P_2W_{17}O_{61}\{O(SiPh)_2\}]\cdot 4H_2O$. Me_2NH_2-**3** is very soluble in acetonitrile and dimethyl sulfoxide, soluble in water, acetone, and methanol, slightly soluble in ethanol, and insoluble in diethyl ether. The solid sample gradually became blue upon exposure to light and is slightly hygroscopic. $(Me_2NH_2)_6[\alpha_2\text{-}P_2W_{17}O_{61}\{O(SiPh)_2\}]\cdot xH_2O$ (x = 0), $C_{24}H_{58}N_6O_{62}Si_2P_2W_{17}$ (4666.1): calcd. C 6.18, H 1.25, N 1.80, P 1.33, Si 1.20, W 66.98; found C 6.15, H 1.23, N 1.81, P 1.29, Si 1.31, W 66.5. A weight loss of 1.91% was observed during the course of overnight drying at room temperature and 10^{-3}–10^{-4} Torr before the analyses, which suggests the presence of between five and six weakly solvated or adsorbed water molecules. TG/DTA under atmospheric conditions: a weight loss of 1.62% with an endothermic point at 83 °C was observed below 201 °C; calcd. 1.52% for x = 4 in $(Me_2NH_2)_6[\alpha_2\text{-}P_2W_{17}O_{61}\{O(SiPh)_2\}]\cdot xH_2O$. The number of solvated or adsorbed water molecules determined by TG/DTA was slightly different from that measured by Pascher (Germany) because the TG/DTA data are dependent on the conditions before analysis. Here, we used four water molecules for the X-ray crystal analysis. IR (KBr disk): $\tilde{\nu}$ = 1617 (s), 1507 (w), 1466 (s), 1430 (w) [PhSi], 1133 (m) [PhSi], 1091 (vs), 1040 (s), 1026 (m), 1017 (m), 960 (s), 952 (s), 925 (m), 904 (w), 795 (vs, br.), 710 (w), 622 (w), 603 (m), 566 (w), 549 (m), 526 (m), 484 (m), 474 (w), 445 (w), 441 (w), 436 (w), 418 (w) cm^{-1}. ^1H NMR (23.0 °C, D_2O): δ = 2.76 (Me_2NH_2), 7.53–7.94 (Ph) ppm. ^{13}C NMR (25.7 °C, D_2O): δ = 37.6 (Me_2NH_2) 131.1–137.3 ppm (Ph). ^{31}P NMR (22.2 °C, D_2O): δ = –10.21, –13.29 ppm.

X-ray Crystallography: Crystals of compounds Me_2NH_2-(**1**–**3**) were covered with liquid paraffin to prevent their degradation. The crystal sizes were 0.11 × 0.11 × 0.07 mm, 0.10 × 0.09 × 0.03 mm, and 0.20 × 0.11 × 0.03 mm, respectively. Data collection was carried out with a Bruker SMART APEX CCD diffractometer at 90 K. The intensity data were automatically corrected for Lorentz and polarization effects during integration. The structure was obtained by direct methods (SHELXS-97),[26] followed by a subsequent difference Fourier calculation, and refined by the full-matrix least-squares procedure (SHELXL-97).[27] Absorption correction was performed with SADABS (empirical absorption correction).[28]

Crystal Data for Me_2NH_2-1: $C_{10}H_{42}N_2O_{68}P_2S_2Si_2W_{17}$, M = 4586.15, monoclinic, space group $P2_1/n$, a = 15.100(4), b = 21.373(5), c = 24.498(6) Å, α = 90°, β = 92.511(4)°, γ = 90°, V = 7898(3) Å^3, Z = 4, D_c = 3.857 Mg m^{-3}, μ(Mo-K_α) = 24.871 mm^{-1}. R_1 = 0.0727, wR_2 = 0.1554 (for all data). R_{int} = 0.0579, R_1 = 0.0562, wR_2 = 0.1447, GOF = 1.071 [92569 total reflections, 19693 unique reflections with $I > 2\sigma(I)$]. The maximum and minimum residual densities (12.244 and –2.629 e Å^{-3}) were located at 1.34 Å from O1 and 0.58 Å from W9, respectively.

Crystal Data for Me_2NH_2-2: $C_{20}H_{66}N_8O_{65}P_2S_2Si_2W_{17}$, M = 4766.50, triclinic, space group $P\bar{1}$, a = 13.2879(12), b = 13.3218(12), c = 26.190(2) Å, α = 80.868(2)°, β = 80.562(2)°, γ = 66.9000(10)°, V = 4183.8(7) Å^3, Z = 2, D_c = 3.784 Mg m^{-3}, μ(Mo-K_α) = 23.483 mm^{-1}. R_1 = 0.0796, wR_2 = 0.1803 (for all data). R_{int} = 0.1890, R_1 = 0.0612, wR_2 = 0.1637, GOF = 0.983 [59851 total reflections, 20747 unique reflections where $I > 2\sigma(I)$]. The maximum and minimum residual densities (10.686 and –4.776 e Å^{-3}) were located at 1.34 Å from O1 and 0.97 Å from W13, respectively.

Crystal Data for Me_2NH_2-3: $C_{22}H_{58}N_5O_{66}P_2Si_2W_{17}$, M = 4692.30, orthorhombic, space group $Pnma$, a = 20.894(4), b = 20.413(4), c = 18.939(3) Å, α = 90°, β = 90°, γ = 90°, V = 8077(3) Å^3, Z = 4, D_c = 3.859 Mg m^{-3}, μ(Mo-K_α) = 24.274 mm^{-1}. R_1 = 0.0534, wR_2 = 0.1168 (for all data). R_{int} = 0.0736, R_1 = 0.0386, wR_2 = 0.1026, GOF = 1.080 [108211 total reflections, 10317 unique reflections where $I > 2\sigma(I)$]. The maximum and minimum residual densities (6.824 and –1.646 e Å^{-3}) were located at 1.34 Å from O1 and 1.57 Å from O26, respectively.

For compound Me_2NH_2-**1**, 17 tungsten atoms, two phosphorus atoms, two silicon atoms, six carbon atoms, and two sulfur atoms were clearly identified. For compound Me_2NH_2-**2**, 17 tungsten atoms, two phosphorus atoms, two silicon atoms, eight carbon atoms, two nitrogen atoms, and two sulfur atoms were clearly identified. For compound Me_2NH_2-**3**, 17 tungsten atoms, two phosphorus atoms, two silicon atoms, and twelve carbon atoms were clearly identified. However, the resolution obtained for the structure of the salt was limited by the poor quality of the available crystals and by the considerable disorder of the countercations and the solvent of crystallization. These features are common in POM crystallography.[29]

CCDC-604936, -604937, and -604938 [Me_2NH_2-(**1**–**3**), respectively] contain the supplementary crystallographic data for this paper. These data can be obtained free of charge from The Cambridge Crystallographic Data Centre via www.ccdc.cam.ac.uk/data_request/cif.

Supporting Information (see the footnote on the first page of this article): The bond lengths, bond angles, and bond valence sums for compounds Me_2NH_2-(**1**–**3**) (Tables S1–S6).

Acknowledgments

This work was supported by Grant-in Aid for Scientific Research (C) no. 18550062 and a High-Tech Research Center Project, both from the Ministry of Education, Culture, Sports, Science and Technology, Japan.

[1] a) M. T. Pope, *Heteropoly and Isopoly Oxometalates*, Springer-Verlag, Berlin, **1983**; b) M. T. Pope, A. Müller, *Angew. Chem. Int. Ed. Engl.* **1991**, *30*, 34–48; c) *Polyoxometalates: From Platonic Solids to Ant-Retrociral Activity* (Eds.: M. T. Pope, A. Müller), Kluwer Academic Publishers, Dordrecht, The Netherlands, **1994**; d) *Chem. Rev.* **1998**, *98*, 1–390 (special issue on polyoxometalates; C. L. Hill, guest editor).
[2] G. Sazani, M. T. Pope, *Dalton Trans.* **2004**, 1989–1994.
[3] a) F. Zonnevijlle, M. T. Pope, *J. Am. Chem. Soc.* **1979**, *101*, 2731–2732; b) G. S. Chorghade, M. T. Pope, *J. Am. Chem. Soc.* **1987**, *109*, 5134–5138; c) W. H. Knoth, *J. Am. Chem. Soc.* **1979**, *101*, 2211–2213.
[4] S. Bareyt, S. Piligkos, B. Hasenknopf, P. Gouserh, E. Laeôte, S. Thorimbert, M. Malacria, *J. Am. Chem. Soc.* **2005**, *127*, 6788–6794.
[5] F. Xin, M. T. Pope, *Organometallics* **1994**, *13*, 4881–4886.
[6] F. Xin, M. T. Pope, G. J. Long, U. Russo, *Inorg. Chem.* **1996**, *35*, 1207–1213.
[7] F. Xin, M. T. Pope, *Inorg. Chem.* **1996**, *35*, 5693–5695.
[8] C. R. Mayer, R. Thouvenot, *J. Chem. Soc., Dalton Trans.* **1998**, 7–13.
[9] G. S. Kim, K. S. Hagen, C. L. Hill, *Inorg. Chem.* **1992**, *31*, 5316–5324.
[10] C. R. Mayer, P. Herson, R. Thouvenot, *Inorg. Chem.* **1999**, *38*, 6152–6158.

[11] C. R. Mayer, M. Hervè, H. Lavanant, J.-C. Blais, F. Sécheresse, *Eur. J. Inorg. Chem.* **2004**, 973–977.
[12] a) P. Judeinstein, C. Deprun, L. Nadjo, *J. Chem. Soc., Dalton Trans.* **1991**, 1991–1997; b) W. H. Knoth, *J. Am. Chem. Soc.* **1979**, *101*, 759–760.
[13] C. R. Mayer, C. Roch-Marchal, H. Lavanant, R. Thouvenot, N. Sellier, J.-C. Blais, F. Sécheresse, *Chem. Eur. J.* **2004**, *10*, 5517–5523.
[14] C. Cannizzo, C. R. Mayer, F. Sécheresse, C. Larpent, *Adv. Mater.* **2005**, *17*, 2888–2892.
[15] A. Mazeaud, Y. Dromzee, R. Thouvenot, *Inorg. Chem.* **2000**, *39*, 4735–4740.
[16] C. R. Mayer, R. Thouvenot, T. Lalot, *Macromolecules* **2000**, *33*, 4433–4437.
[17] D. Agustin, C. Coelho, A. Mazeaud, P. Herson, A. Proust, R. Thouvenot, *Z. Anorg. Allg. Chem.* **2004**, *630*, 2049–2053.
[18] A. Maseaud, N. Ammari, F. Robert, R. Thouvenot, *Angew. Chem. Int. Ed. Engl.* **1996**, *35*, 1961–1964.
[19] N. Ammari, G. Hervè, R. Thouvenot, *New J. Chem.* **1991**, *15*, 607–608.
[20] J. Niu, M. Li, J. Wang, *J. Organomet. Chem.* **2003**, *675*, 84–90.
[21] C. R. Mayer, S. Neveu, V. Cabuil, *Angew. Chem. Int. Ed.* **2002**, *41*, 501–503.
[22] Y. Sakai, A. Shinohara, K. Hayashi, K. Nomiya, *Eur. J. Inorg. Chem.* **2006**, 163–171.
[23] a) I. D. Brown, D. Altermatt, *Acta Crystallogr., Sect. B* **1985**, *41*, 244–247; b) I. D. Brown, R. D. Shannon, *Acta Crystallogr., Sect. A* **1973**, *29*, 266–282; c) I. D. Brown, *Acta Crystallogr., Sect. B* **1992**, *48*, 553–572; d) I. D. Brown, *Appl. Cryst.* **1996**, *29*, 479–480.
[24] R. M. Silverstein, G. C. Bassler, T. C. Morrill, *Spectrometric Identification of Organic Compounds*, 5th ed., John Wiley & Sons, Inc., New York, **1991**.
[25] D. K. Lyon, W. K. Miller, T. Novet, P. J. Domaille, E. Evitt, D. C. Johnson, R. G. Finke, *J. Am. Chem. Soc.* **1991**, *113*, 7209–7221.
[26] G. M. Sheldrick, *Acta Crystallogr., Sect. A* **1990**, *46*, 467–473.
[27] G. M. Sheldrick, SHELXL-97, *Program for Crystal Structure Refinement*, University of Göttingen, Germany, **1997**.
[28] G. M. Sheldrick, SADABS, University of Göttingen, Germany, **1996**.
[29] a) K. Nomiya, M. Takahashi, K. Ohsawa, J. A. Widegren, *J. Chem. Soc., Dalton Trans.* **2001**, 2872–2878; b) T. J. R. Weakley, R. G. Finke, *Inorg. Chem.* **1990**, *29*, 1235–1241; c) Y. Lin, T. J. R. Weakley, B. Rapko, R. G. Finke, *Inorg. Chem.* **1993**, *32*, 5095–5101; d) T. Yamase, T. Ozeki, H. Sakamoto, S. Nishiya, A. Yamamoto, *Bull. Chem. Soc. Jpn.* **1993**, *66*, 103–108; e) K. Nomiya, M. Takahashi, J. A. Widegren, T. Aizawa, Y. Sakai, N. C. Kasuga, *J. Chem. Soc., Dalton Trans.* **2002**, 3679–3685.

Received: May 23, 2006
Published Online: October 12, 2006

